RSC Advances

Ultrasensitive tactile sensors based on planar liquid crystal-gated-organic field-effect transistor with polymeric dipole control layer

Journal:	*RSC Advances*
Manuscript ID:	RA-COM-05-2015-008921.R1
Article Type:	Communication
Date Submitted by the Author:	05-Jun-2015
Complete List of Authors:	Seo, Jooyeok; Kyungpook National University, Department of Chemical Engineering Song, Myeonghun; Kyungpook National University, Department of Chemical Engineering Han, Hyemi; Kyungpook National University, Department of Chemical Engineering Kim, Hwajeong; Kyungpook Nationa University, Research Institute for Advanced Energy Technology Lee, Joon-Hyung; Kyungpook National University, School of Materials Science & Engineering Park, Soo-Young; Kyungpook National University, Department of Polymer Science Kang, Inn-Kyu; kyung pook national university, department of polymer science and engineering Kim, YoungKyoo; Kyungpook National University, Department of Chemical Engineering

Journal Name

COMMUNICATION

Ultrasensitive tactile sensors based on planar liquid crystal-gated-organic field-effect transistor with polymeric dipole control layer

Received 00th January 20xx,
Accepted 00th January 20xx

DOI: 10.1039/x0xx00000x

www.rsc.org/

Jooyeok Seo,[a] Myeonghun Song,[a] Hyemi Han,[a] Hwajeong Kim,[a,b,*] Joon-Hyung Lee,[c] Soo-Young Park,[d] Inn-Kyu Kang,[d] and Youngkyoo Kim[a,*]

A polymeric dipole control layer (DCL) greatly reduced the leakage current in planar liquid crystal-gated-organic field-effect transistors and the resulting LC-DCL-g-OFET devices could detect extremely low intensity of nitrogen gas flows which cannot be felt by human skins.

A touch sensor has been one of the important technologies in the present electronics era which is often represented by smart phones and smart pads.[1-5] In addition to such electronics fields, touch sensors are coming up as a key component for robots, particularly humanoid robots which resemble humans in their shape, because they plays a critical role in sensing as an artificial skin for robots like a human skin.[6-10] However, most of previously reported touch sensors for artificial skins are sensitive to the direct physical touch, because the sensing mechanism is based on the resistive and/or capacitive signal changes[11-15], but cannot sense weak air flows induced by the movement of neighboring objects even though this induced tactile sensing function is of crucial importance in the self-protection against approaching objects and in the determination of next actions.

Very recently, our group have reported such induced tactile sensing devices by employing a liquid crystal (LC) as a sensing layer in the structure of organic field-effect transistors (OFETs): LC-on-OFET and LC-g-OFET.[16-18] We note that LC-on-OFET has the LC sensing layer on top of the channel layer of typical OFET with bottom source/drain electrodes but LC-g-OFET features a planar transistor structure with the LC layer that plays a dual role (both sensing and gate insulator). The LC-on-OFET devices could detect very low intensity of nitrogen flows, which cannot be felt by human skins, while an external touch was sensitively detected by the LC-g-OFET devices. However, it was a drawback for both LC-on-OFET and LC-g-OFET devices that the surface of active (channel) layers, which does directly contact the LC layer, was affected by the dipoles of LC molecules leading to the generation of charges in the channel layer. As a consequence, the leakage current was inevitably high even at zero gate voltage condition, which resulted in the poor OFF current in the devices.

In this communication, a new device structure with a dipole control layer (DCL), which is inserted between the channel layer and the LC layer, is proposed in order to prevent the generation of charges in the channel layer at zero gate electric field, since the insertion of DCL can avoid the direct contact between the surface of channel layer and the LC layer. Here poly(methyl methacrylate) (PMMA) was employed as a DCL because of the electrical insulating characteristics of PMMA.[19,20]

As illustrated in Fig. 1a (bottom), it is considered that the positive charges (holes) are not generated by the presence of DCL because the PMMA layer (DCL) blocks the induction effect by the native dipole of LC molecules when no strong external electric field is applied across the DCL. This idea is certainly proved from the current – voltage (I-V) curves in Fig. 1b (left) because the device current in the planar diode structure was remarkably (>100-fold) reduced by introducing the 10 nm-thick PMMA DCL between the channel layer (poly(3-hexylthiophene) - P3HT) and the LC layer (4-cyano-4'-pentylbiphenyl - 5CB): Note that the dielectric constant of PMMA and 5CB is 3.5 and 18 (nematic phase), respectively.[20,12] The pronounced blocking (rectification) effect is also attributed to the good quality of the PMMA layer, which is observed from the atomic force microscope (AFM) images in Fig. 2b (right), because a considerable amount of leakage current might be measured in the case of pinhole-like defects made in the PMMA layer. It is

[a.] *Organic Nanoelectronics Laboratory, School of Applied Chemical Engineering, Kyungpook National University, Daegu 702-701, Republic of Korea. (E-mail: ykimm@knu.ac.kr)*
[b.] *Priority Research Center, Research Institute of Advanced Energy Technology, Kyungpook National University, Daegu 702-701, Republic of Korea. (E-mail: khj217@knu.ac.kr)*
[c.] *School of Materials Science and Engineering, Kyungpook National University, Daegu 702-701, Republic of Korea.*
[d.] *Department of Polymer Science and Engineering and Graduate School of Applied Chemical Engineering, Kyungpook National University, Daegu 702-701, Republic of Korea.*
† Electronic Supplementary Information (ESI) available*: photographs for the LC spreading, drain current change at 3 s stimulation, illustration for the negative dipole end of 5CB, brightness-enhanced POM images, and experimental details*. See DOI: 10.1039/x0xx00000x

also worthy to note that the spreading characteristics of 5CB drop were greatly enhanced on the PMMA layer, which may be ascribed to both the noticeable reduced surface roughness and intrinsic surface property of the PMMA layer compared to the P3HT layer (see Fig. S1).

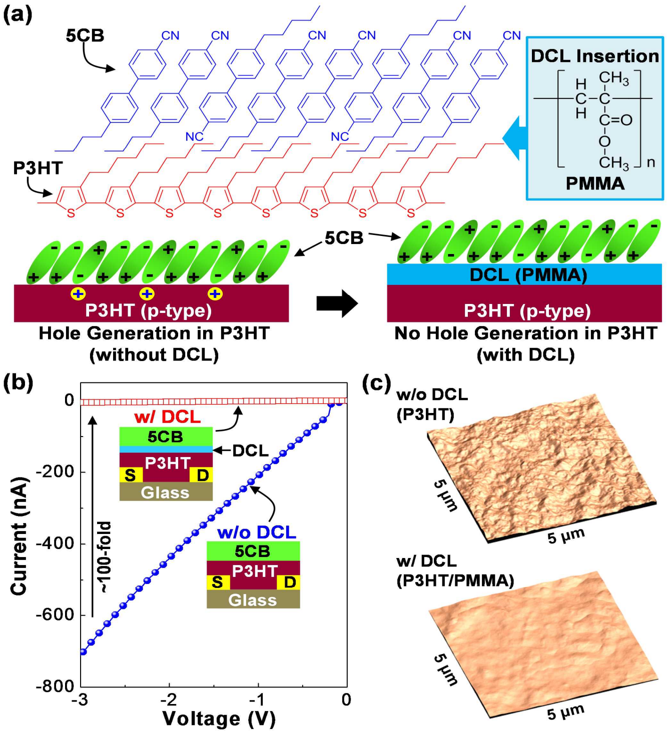

Fig. 1 (a) Illustration for the concept of DCL (PMMA) insertion (top) leading to the blocking of charge generation in the channel (P3HT) layer (bottom). (b) Current – voltage (I-V) curves for the planar diode structure with and without the DCL. (c) Height-mode AFM images (5µm x 5µm) for the surface of the channel (P3HT) layer (top) and the DCL (PMMA) layer (bottom).

After checking the proposed idea that showed the significantly reduced leakage current (see Fig. 1b), the planar LC-g-OFET devices were fabricated by inserting the PMMA DCL between the channel (P3HT) layer and the LC (5CB) layer (see Fig. 2a), which is called "LC-DCL-g-OFET" hereafter. As shown in the output curves (Fig. 2b (left)), the present LC-DCL-g-OFET devices exhibited a p-type field-effect transistor behaviour because of the gradual (negative) drain current (I_D) increase with the (negative) drain voltage (V_D) at a fixed gate voltage (V_G) and the proportional drain current jump with the gate voltage at a fixed drain voltage. Additional p-type transistor behaviour is also observed clearly from the transfer curves because the steep (negative) increase was measured in the drain current as the gate voltage increased in the negative direction at a fixed drain voltage (V_D = -1 V). Considering this obvious p-type transistor behaviour, the PMMA DCL is regarded to participate in the induced polarization process leading to the formation of positive charges in the P3HT layer as illustrated in Fig. 2a. Here a particular attention is paid to the low OFF current (~10 pA) leading to the high ON/OFF ratio (>10^4) and the stiff, which is better than the previous results for the LC-g-OFET device with the DCL.[16]

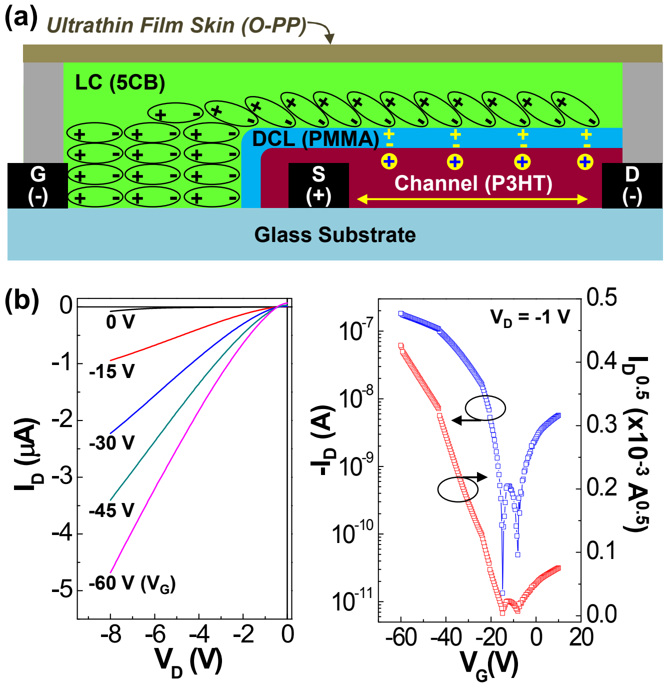

Fig. 2 (a) Illustration for the planar LC-g-OFET device with the PMMA DCL (LC-DCL-g-OFET): The dipole direction of LC (5CB) molecules is schematically expressed under applied electric fields ($|V_G| > |V_D|$, $V_G < 0$ V, $V_D < 0$ V). (b) Output (left) and transfer (right) curves for the planar LC-g-OFET device with the PMMA DCL.

Next, the LC-DCL-g-OFET devices were examined by applying weak nitrogen gas flows as an external stimulation (see Fig. 3a).[11-13] As shown in Fig. 3b, the turn-on of nitrogen flows initialized the gradual increase of drain current to a maximum value and then the turn-off (after 20 s) of nitrogen flows resulted in the decay of drain current irrespective of the intensity of nitrogen flows. This behaviour can be related to the dynamic motion of LC molecules in the present device structure. Here it is worthy to note that the present LC-DCL-g-OFET devices could sense such a low gas intensity (0.5 sccm = ~8.3 µl/s), which is slightly lower than the low limit of previously reported gas intensity (~11 µl/s) measured by LC-on-OFET devices.[16] This result supports that the present LC-DCL-g-OFET devices are indeed ultrasensitive in terms of nitrogen gas intensity and can be applied for the sensation of extremely low intensity gas flows. Here it is noted that the level of sensing currents compared to base currents is quite low owing to the presence of the polymer film skin, which can be further improved by controlling the thickness and/or kind of polymer skins. As shown in Fig. 3c, the overall response or duration time (**t**$_D$) of sensing signals was noticeably varied with the stimulation time of nitrogen flows at the same intensity. When the stimulation time was 3 s, the duration time of signal was less than 6 s. However, as the stimulation time increased, the duration time has a tendency to be short in the case of rapid decay part in the drain current signals. However, the duration time was almost identical at the same stimulation time even though the intensity of nitrogen flows was changed, whereas the drain current was almost linearly increased with the gas intensity (strength) irrespective of the stimulation time (see Fig. S2 for the case of 3 s stimulation).

Considering the trend of drain current upon stimulation of nitrogen flows in Fig. 3bc, it is obvious that the drain current was negatively increased by the stimulation of nitrogen flows. This provides us with a mechanism on the present LC-DCL-g-OFET devices in the case of gas flow detection: When the nitrogen flow was applied to the top film skin part of the LC-DCL-g-OFET devices (Fig. 3a), the part stimulated by the nitrogen flow could be deformed depending on the strength of nitrogen flows. As a consequence, the LC (5CB) molecules are supposed to be fluctuated leading to the change in the polarization direction, in which the negative end of the 5CB molecules might actually affect the surface of the PMMA layer (DCL) when it comes to the structure of 5CB molecule (see Fig. S3).

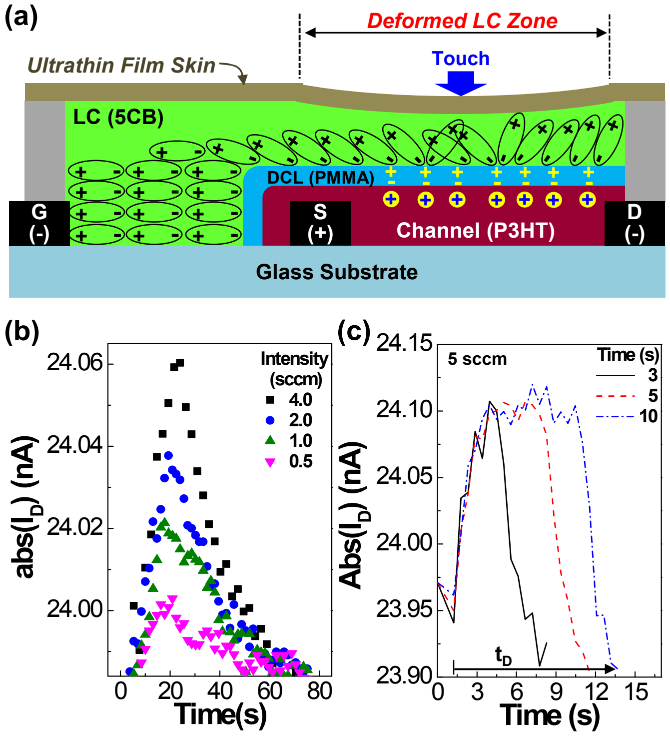

Fig. 3 (a) Illustration for the fluctuation of the LC layer in the planar LC-DCL-g-OFET device upon stimulation of external touch (nitrogen flow) at V_G = -5 V and V_D = -0.5 V. (b) Drain current as a function of time upon stimulation of nitrogen flows at various intensities (note that the stimulation time was 20 s). (c) Drain current as a function of time upon stimulation of nitrogen flow (5 sccm) by varying the stimulation time from 3 s to 20 s (the total duration time (**t**$_D$) is marked for example).

To confirm the mechanism suggested from the trend of drain current, a polarized optical microscopy (OM) was employed to examine the states of 5CB molecules according to various conditions. As shown in Fig. 4 (top left), a medium brightness at the linear polarization condition (0^o) was measured in the channel region in the case of no electric fields and no nitrogen flows. However, the channel region at the crossed polarization condition (90^o) was almost dark in the presence of partly lighted parts with very low intensity (see the brightness controlled images in Fig. S4). This result informs that the 5CB molecules made a very slightly tilted (ca. 80^o) homeotropic alignment on top of the PMMA DCL in the present device structure. In particular, it is worthy to note that the extent of the tilted 5CB molecules on the PMMA DCL is relatively smaller than that on the P3HT layer.[16] However, when both gate and drain voltages (V_G = -5 V and V_D = -0.5 V) were applied, the channel area became much brighter at 0^o and much darker at 90^o compared to the no bias condition (see the middle images in Fig. 4). So it is supposed that the 5CB molecules underwent a preferential alignment in the gate-source-drain (G-S-D) direction under the electric field (V_G = -5 V and V_D = -0.5 V) even though a marginal tilted part might be present depending on the conditions of the DCL surfaces and/or the geometry of the ITO electrodes.

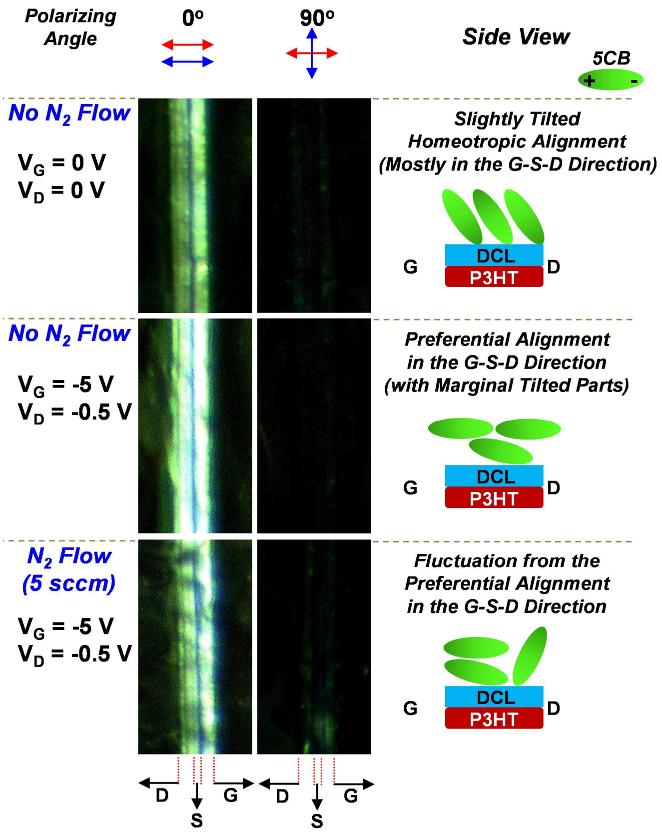

Fig. 4 Optical microscope images focused on the channel area in the LC-DCL-g-OFET device according to various conditions (with and without electric fields and/or nitrogen flows). The polarizing angle accounts for the combination of two linear polarizers. A possible state of LC molecules is given on the right part. Note that the net electric field between the gate electrode and the drain electrode is $V_G - V_D < 0$ V.

Next, when the nitrogen flow was applied to the LC-DCL-g-OFET device at V_G = -5 V and V_D = -0.5 V, the brightness in the channel region was unevenly changed and relatively reduced as observed from the OM image (0^o) in Fig. 4 (bottom left). Interestingly, the brightness in the channel area was very slightly increased at 90^o (see better comparison in Fig. S4), which indicates that the preferential LC alignment in the G-S-D direction was partly broken by the stimulation of nitrogen flows. This broken alignment is an evidence for the fluctuation of 5CB molecules under the stimulation of nitrogen flows, which gave rise to the generation of more positive charges in the channel layer (see Fig. 3a) as supported by the (negatively) increased drain current (see Fig. 3bc).

Conclusions

In conclusion, the dielectric control layer (DCL) was introduced in order to reduce the intrinsic leakage current by the direct contact between the LC layer and the channel layer in the LC-g-OFET devices. The insertion of the 10 nm-thick PMMA DCL resulted in remarkably reduced leakage current by more than 100-fold, which was attributed to the well formation of the PMMA layer as supported by the AFM measurement. The LC-g-OFET device with the DCL, so-called LC-DCL-g-OFET, showed good p-type transistor behaviour with a low OFF current (< 10 pA). The LC-DCL-g-OFET devices were sensitively and systematically responded to the stimulation of nitrogen gas flows, while they could detect extremely low intensity of nitrogen flow (0.5 sccm = ~ 8.3 μl/s) which cannot be properly felt by human skins. The response (signal duration) time was dependent on the stimulation time of nitrogen flows, whereas it was almost independent on the intensity (strength) of the nitrogen flow. The fluctuation of LC molecules in the channel layer, leading to the increased contact of the negative (dipole) end of LC molecules to the surface of the channel layer, has been assigned to the core mechanism for the sensation of weak gas (nitrogen) flows by the LC-DCL-g-OFET devices.

Acknowledgements

This work was financially supported by the grants from Korean Government (Basic Research Laboratory Program_2011-0020264, Basic Science Research Program_2009-0093819, NRF_2012K1A3A1A09027883, MOTIE_10048434, NRF_2014R1-A1A3051165, Human Resource Training Project for Regional Innovation_MOE(NRF_2014H1C1A1066748, NRF_2014H1-AA2A1016454)).

Notes and references

1 H. Tian, D. Xie, Y. Yang, T.-L. Ren, Y.-F. Wang, C.-J. Zhou, P.-G. Peng, L.-G. Wang and L.-T. Liu, *Nanoscale,* 2012, **4**, 3345.
2 A. D. Mazzeo, W. B. Kalb, L. Chan, M. G. Killian, J.-F. Bloch, B. A. Mazzeo and G. M. Whitesides, *Adv. Mater.,* 2012, **24**, 2850.
3 M. Segev-Bar, A. Landman, M. Nir-Shapira, G. Shuster and H. Haick, *ACS Appl. Mater. Interfaces,* 2013, **5**, 5531.
4 S. Chun, Y. Kim, H. Jung and W. Park, *Appl. Phys. Lett.,* 2014, **105**, 041907.
5 S. Takamatsu, T. Yamashita, T. Imai and T. Itoh, *Sensors Actuators A: Phys.,* 2014, **220**, 153.
6 W. Wu, X. Wen and Z. L. Wang, *Science,* 2013, **340**, 952.
7 C. Hou, T. Huang, H. Wang, H. Yu, Q. Zhang and Y. Li, *Sci. Rep.,* 2013, **3**, 3138.
8 C. Wang, D. Hwang, Z. Yu, K. Takei, J. Park, T. Chen, B. Ma and A. Javey, *Nat. Mater.,* 2013, **12**, 899.
9 G. Zhu, W. Q. Yang, T. Zhang, Q. Jing, J. Chen, Y. S. Zhou, P. Bai and Z. L. Wang, *Nano Lett.,* 2014, **14**, 3208.
10 H.-K Kim, S. Lee and K.-S. Yun, *Sensors Actuators A: Phys.,* 2011, **165**, 2.
11 S. Kim, W. Choi, W. Rim, Y. Chun, H. Shim, H. Kwon, J. Kim, I. Kee, S. Kim, S. Lee and J. Park, *IEEE Trans. Electron Devices.,* 2011, **58**, 3609.
12 L. Bürgi, R. Pfeiffer, M. Mücklich, P. Metzler, M. Kiy and C. Winnewisser, *Org. Electron.,* 2006, **7**, 114.
13 H. Tian, Y. Shu, X.-F. Wang, M. A. Mohammad, Z. Bie, Q.-Y. Xie, C. Li, W.-T. Mi, Y. Yang and T.-L. Ren, *Sci. Rep.,* 2015, **5**, 8603.
14 X. Lee, T. Yang, X. Li, R. Zhang, M. Zhu, H. Zhang, D. Xie, J. Wei, M. Zhong, K. Wang, D. Wu, Z. Li and H. Zhu, *Appl. Phys. Lett.,* 2013, **102**, 163117.
15 J. Seo, S. Park, S. Nam, H. Kim and Y. Kim, *Sci. Rep.,* 2013, **3**, 2452.
16 J. Seo, C. Lee, H. Han, S. Lee, S. Nam, H. Kim, J.-H. Lee, S.-Y. Park, I.-K. Kang and Y. Kim, *AIP Adv.,* 2014, **4**, 097109.
17 J. Seo, S. Nam, J. Jeong, C. Lee, H. Kim and Y. Kim, *ACS Appl. Mater. Interfaces,* 2015, **7**, 504.
18 G.-W. Kang, K.-M. Park, J.-H. Song, C. Lee and D. Hwang, *Curr. Appl. Phys.,* 2005, **5**, 297.
19 J. Veres, S. Ogier, G. Lloyd and D. de Leeuw, *Chem. Mater.,* 2004, **16**, 4543.
20 Y. Hisakado, H. Kikuchi, T. Nagamura and T. Kajiyama, *Adv. Mater.,* 2005, **17**, 96.